

# Uncertainty-Aware Adapter: Adapting Segment Anything Model (SAM) for Ambiguous Medical Image Segmentation

Mingzhou Jiang<sup>1,\*</sup>, Jiaying Zhou<sup>1,\*</sup>, Junde Wu<sup>2,\*†</sup>, Tianyang Wang<sup>1</sup>, Yueming Jin<sup>3</sup>, and Min Xu<sup>4,✉</sup>

\* equal technical contribution † project lead

<sup>1</sup> University of Alabama at Birmingham

<sup>2</sup> University of Oxford

<sup>3</sup> National University of Singapore

<sup>4</sup> Carnegie Mellon University

mxu1@cs.cmu.edu

**Abstract.** The Segment Anything Model (SAM) gained significant success in natural image segmentation, and many methods have tried to fine-tune it to medical image segmentation. An efficient way to do so is by using Adapters, specialized modules that learn just a few parameters to tailor SAM specifically for medical images. However, unlike natural images, many tissues and lesions in medical images have blurry boundaries and may be ambiguous. Previous efforts to adapt SAM ignore this challenge and can only predict distinct segmentation. It may mislead clinicians or cause misdiagnosis, especially when encountering rare variants or situations with low model confidence. In this work, we propose a novel module called the Uncertainty-aware Adapter, which efficiently fine-tuning SAM for uncertainty-aware medical image segmentation. Utilizing a conditional variational autoencoder, we encoded stochastic samples to effectively represent the inherent uncertainty in medical imaging. We designed a new module on a standard adapter that utilizes a condition-based strategy to interact with samples to help SAM integrate uncertainty. We evaluated our method on two multi-annotated datasets with different modalities: LIDC-IDRI (lung abnormalities segmentation) and REFUGE2 (optic-cup segmentation). The experimental results show that the proposed model outperforms all the previous methods and achieves the new state-of-the-art (SOTA) on both benchmarks. We also demonstrated that our method can generate diverse segmentation hypotheses that are more realistic as well as heterogeneous.

**Keywords:** SAM · Adapter · uncertainty · samples.

## 1 Introduction

Medical image segmentation plays a vital role in healthcare, offering crucial insights for various downstream clinician applications, like disease diagnosis and

evaluation. Recently, many proposed to adapt the pre-trained nature image segmentation model, like Segment Anything Model (SAM) [1] to medical image segmentation [2, 3, 4]. A popular cost-efficient approach is the Adapter technique, which involves inserting a bottleneck module with only a few parameters into the model. Through fine-tuning these small-size adapters, SAM can bridge the domain gap between medical and natural images while retaining superior performance. For instance, MSA [5], SAM-Med2D [6], SAM-adapter [7], and others employ an Adapter strategy to transfer SAM to medical imaging, achieving superior segmentation results.

However, unlike natural images, medical images have the unique features that many organs and tissues in medical images are ambiguous. For example, when segmenting lesions from lung abnormality images, different clinicians are likely to provide varied annotations, and it is common to combine these different annotations to represent the final ground truth with inherent uncertainty. Conventional computer vision models, like SAM, are challenging to apply directly in such cases. They tend to output the one-to-one mapping from image to ground truth, which may lead to mispredictions and potentially mislead clinicians' diagnoses. Previous efforts to adapt SAM to the medical field have also overlooked this critical challenge, rendering them inapplicable for many real-world clinical scenarios. Therefore, for fine-tuning SAM to medical images, it is essential to present a new fine-tuning method that helps the model understand and calibrate uncertainty-aware segmentation.

In this paper, we propose a novel module called the Uncertainty-aware Adapter for fine-tuning SAM to ambiguous medical image segmentation. The basic idea is to construct a latent space for sampling the possible segmentation variants following the previous uncertainty works like Probabilistic U-Net (Prob U-Net) [8, 9, 10] so that SAM can interact with the stochastic samples. Unlike most previous works in the stochastic sample, which is merely applied to the output layer of the model by concatenation, we design a new interaction method between the model and samples to overcome the issue where the model might ignore samples. In order to adapt this idea of sampling to our specific case that the Adapters only contain a few parameters, we propose the Uncertainty-aware Adapter, which utilizes a condition-based strategy to interact with uncertainty samples from latent space. We designed a novel module called Condition Modifies Sample Module (CMSM) in the Uncertainty-aware Adapter to learn the interaction between the uncertainty sample and the Adapter. The learnable position variant of the Uncertainty-aware Adapter matches the feature-extracting process and is treated as the condition to calculate with the uncertainty sample. Our method enhances interaction with uncertainty samples, yielding more diverse and accurate segmentations.

Our contributions can be summarized as follows:

- We present the Uncertainty-aware Adapter SAM(UA-SAM), which combines a probabilistic model to produce diverse likely segmentation hypotheses. It is crucial to provide clinicians with reliable diagnostic assistance and reduce the risk of misdiagnosis.

- We proposed the Condition Modifies Sample Module (CMSM) in the Uncertainty-aware Adapter, which can help SAM to capture the uncertainty in medical images while segmenting ambiguous medical images.
- We have evaluated our proposed UA-SAM model on the LIDC-IDRI dataset and the REFUGE dataset. Our method demonstrates superior segmentation performance, a significant step in ambiguous medical image segmentation.

## 2 Method

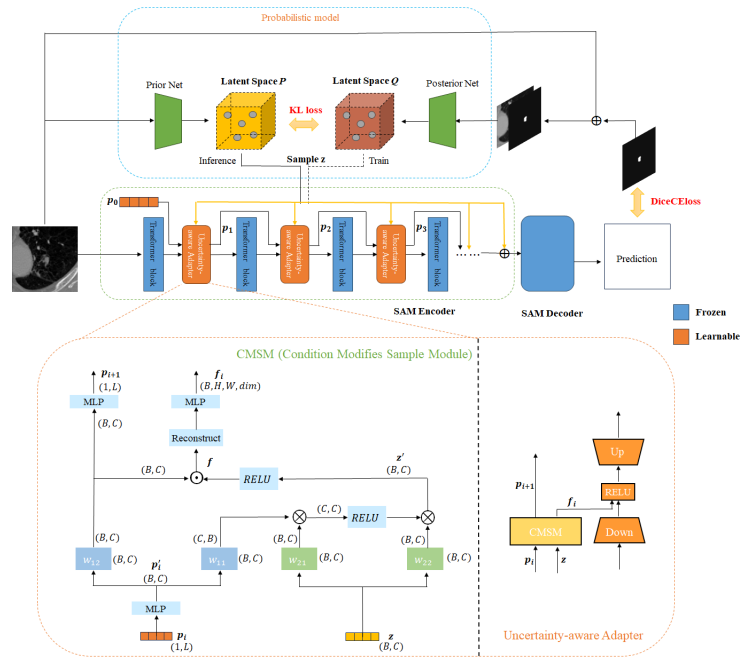


**Fig. 1.** Overview of UA-SAM. We froze the parameters of SAM and only updated the Adapter parameters. Note that we did not show the prompt encoder.

Before introducing UA-SAM, we provide an overview of the SAM architecture. SAM consists of three main components: a large-scale image encoder, a prompt encoder, and a lightweight mask decoder. The image encoder utilizes a Vision Transformer (ViT) pre-trained by MAE [11] to process high-resolution images (default  $1024 \times 1024$ ). The output embeddings of the image encoder are at  $1/16$  scale of the input image. The prompt encoder has two prompt styles: sparse (points, boxes, texts) and dense (masks). Convolutional down-sampling and GELU activation functions are applied to dense prompts. The mask decoder

updates image embeddings and prompt embeddings via two-way cross attention, from prompt to image and image to prompt. This SAM framework allows it to segment different targets based on different prompts.

In our work, we propose the Uncertainty-aware Adapter, learning a few parameters while integrating uncertainty, which helps fine-tune SAM to the uncertainty-aware medical image segmentation effectively. We use the probabilistic model to model latent space. The Uncertainty-aware Adapter utilizes a condition-based interaction method between the latent space uncertainty sample and SAM, ensuring the model can output accurate and diverse likely segmentation hypotheses. Our proposed UA-SAM architecture is shown in Fig. 1.

**Overview of UA-SAM.** To output diverse plausible segmentation masks, UA-SAM utilizes a probabilistic model to produce unlimited uncertainty samples, and a segmentation model interacts with samples to output segmentation masks. The probabilistic model inputs the images and models the distribution of images, then outputs uncertainty samples. During the training and inference processes, the probabilistic model provides an uncertainty sample  $z$  for the segmentation model. The segmentation model is the SAM model that is fine-tuned by inserting Adapters into the image encoder. The  $i$ -th ( $i = 0, 1, 2, \dots$ ) Uncertainty-aware Adapter is inserted behind the  $i$ -th Transformer block. All Adapter inputs position variant  $p_i$  and uncertainty sample  $z$ , then outputs  $p_{i+1}$  for the next Adapter (Except for the last adapter, its output is directly added to the embeddings reconstructed from the sample  $z$  to the same dimensionality.).

**Probabilistic model.** Following the previously most commonly used paradigm [8, 9, 10], we utilize a Prior Net and a Posterior Net to separately construct low-dimensional latent spaces  $P$  and  $Q$ , which obey the Gaussian distribution  $\mathcal{N}(\mu, \text{diag}(\sigma))$ . For the training process, the uncertainty sample  $z$  comes from the latent space  $Q$ , and the inference process from the latent space  $P$ , which is a random sample. At the same time, there is a Kullback-Leibler divergence, which is a part of the loss function (in Eq. 6) to penalize differences between the posterior distribution  $Q$  and the prior distribution  $P$ .

**Architecture of Uncertainty-aware Adapter.** In order to reduce the number of fine-tuning parameters as much as possible, the Uncertainty-aware Adapter (as shown in Fig. 1) consists of two small-size components: one is a bottleneck model that sequentially uses a down-projection, ReLU activation, and up-projection, and another is the Condition Modifies Sample Module (CMSM), which designed for interaction between uncertainty sample  $z$  and Adapter. Fig. 1 illustrates CMSM schematically. Given the learnable position variant  $p_i \in \mathbb{R}^{1 \times L}$  ( $L$  is the number of Adapter ) of current Adapter and uncertainty sample  $z \in \mathbb{R}^{B \times C}$  ( $B$  is the batch size  $C$  is the latent space dimension), CMSM utilizes  $p_i$  as the condition to modify the state of  $z$ . It is similar to the dot-product attention [12] using  $p_i$  as the query and  $z$  as the key. This ensures the uncertainty sample matches the feature extraction process so that the model effectively responds to incorporating the uncertainty sample. Concretely, the computational steps of the CMSM mechanism are demonstrated as follows:

$$p_i' = \text{Reshape}(MLP(p_i)) \quad (1)$$

$$z' = w_{22}(z) \otimes \text{ReLU}(\text{Trans}(w_{11}(p_i')) \otimes w_{21}(z)) \quad (2)$$

$$f = \text{ReLU}(z') \odot w_{12}(p_i') \quad (3)$$

$$f_i = MLP(\text{Reconstruct}(f)) \quad (4)$$

$$p_{i+1} = \text{flatten}(MLP(w_{12}(p_i'))) \quad (5)$$

where  $w_{11}$ ,  $w_{12}$ ,  $w_{21}$  and  $w_{22}$  are linear projection function. ‘Trans’ refers to the transposing to transform feature tensors into proper shapes for calculation. Here, ‘ $\otimes$ ’ and ‘ $\odot$ ’ represent matrix multiplication and element-wise multiplication at corresponding positions. And the ‘Reconstruct’ denotes transforming feature tensors from  $f \in \mathbb{R}^{B \times C}$  to  $f \in \mathbb{R}^{B \times H \times W \times \text{dim}}$  ( $H$  and  $W$  are the height and width of patch embeddings processed by image encoder.  $\text{dim}$  is a value of multiplying a ratio and embeddings dimension). The uncertainty sample  $z$  is ultimately modified to the uncertainty feature  $f_i$  that can be directly concatenated with down-projection embeddings. And CMSM also outputs the next position variant  $p_{i+1}$  for the next Adapter.

$$\mathcal{L} = E_{z \sim Q(\cdot | Y, X)} [-\log P_\theta(Y | S(X, z))] + \beta \times D_{KL}(Q(z | Y, X) \| P(z | X)) \quad (6)$$

In the training process, we compute the loss, as shown in Eq. 6. Given the raw image  $X$  and the ground truth segmentation  $Y$ ,  $S$  is the predicted segmentation. A DiceCEloss from the Monai library penalizes differences between  $S$  and  $Y$  (the DiceCEloss arises from treating the output  $S$  as the parameterization of a pixel-wise categorical distribution  $P_\theta$ )

## 3 Experiment

### 3.1 Dataset

We trained and evaluated our model on two multi-annotated datasets with different modalities: the LIDC-IDRI dataset [13] and the REFUGE2 dataset [14]. For the LIDC-IDRI dataset, we use a pre-processed version of the dataset, cropped 128\*128 patches around lesions, which comprises 15096 thoracic CT images with lesions annotated by four radiologists. Moreover, we conducted experiments on the REFUGE2 optic-cup dataset, consisting of 1200 fundus images, each annotated by seven radiologists. Both datasets are publicly available.

For the LIDC-IDRI dataset, we divided the dataset into a training set and a testing set at a ratio of 80:20. The training set comprises 12076 images, while the testing set shall consist of 3018 (drop last), each measuring 128\*128 pixels. For the REFUGE2 optic-cup dataset, we cropped the fundus images around the center of the optic disc and then resized them to the size of 512\*512. Subsequently, we combined the training and validation set into a new one, resulting in 800 images in the training set and 400 images in the testing set.

### 3.2 Implementation details

In this study, we implemented our model on the LIDC-IDRI and REFUGE2 datasets. We utilized the PyTorch and MONAI libraries for our project and employed the Adam optimizer with an initial learning rate set to 1e-4. Meanwhile, we incorporated the StepLR strategy for learning rate decay. During training, the labels were randomly sampled from the multiple annotated labels corresponding to the images. To ensure the highest model efficacy, we implemented a simple, early-stopping mechanism. We use the "vit/b" version of SAM. Additionally, in our training process, SAM was employed with single-point prompts.

**Table 1.** The Comparison of UA-SAM with SOTA methods evaluated by Dice Score. The best results are denoted in bold.

Method		LIDC-IDRI	REFUGE2
Deterministic Method	Unet [15]	0.516	0.726
	nnU-Net [16]	0.846	0.829
	Attention U-Net [17]	0.866	0.846
	TransUNet [18]	0.879	0.835
	R2U-Net [19]	0.851	0.778
	Deeplabv3+ [20]	-	0.846
	SAM	0.157	0.367
	Adapter-SAM	0.861	0.823
Uncertainty Method	Ensemble U-Net	0.557	0.744
	Pro U-Net [8]	0.602	0.682
	UGMCS-Net [21]	0.876	-
	MRNet [22]	0.878	0.849
	UA-SAM(ours)	<b>0.887</b>	<b>0.856</b>

### 3.3 Main results

We compared our UA-SAM model with SOTA segmentation methods, classified into deterministic methods (U-Net, nnU-Net, Attention U-Net, TransUNet, R2U-Net, Deeplabv3+, SAM, Adapter-SAM) and uncertainty methods (Ensemble U-Net, Pro U-Net, UGMCS-Net, MRNet). The segmentation performance was evaluated using the Dice score, with quantitative results in Table. 1. We got our results by using the majority vote strategy to deal with samples and multiple-annotated masks (our model performs the best when it samples 4 times in the LIDC-IDRI dataset and 3 times in the REFUGE2 dataset). Our model outperformed others with the highest Dice score of 88.7% on the LIDC-IDRI dataset and 85.6% on the REFUGE2 dataset.

Additionally, in Table. 1, we compared our method with three related methods, including Pro U-Net, SAM, and Adapter-SAM. It is quite evident that our method has a significant advantage, even though UA-SAM and probabilistic U-Net both utilize the probabilistic model to learn uncertainty. Our method still shows an improvement of 28.5% and 17.4% on two datasets compared with Pro

U-Net. It’s worth mentioning that SAM struggles to cross the domain of these two datasets, even though it has already demonstrated excellent zero-shot capabilities in natural image segmentation. Adapter-SAM(similar to MSA[5], but the position of the Adapter for MSA is inside the Transformer block.) learns the medical domain knowledge via the Adapter and makes a giant improvement of 70.4% and 45.6% on two datasets compared with SAM, but it is 2.6% and 3.3% lower than ours. It demonstrates the Uncertainty-aware Adapter we proposed is more efficient than the normal Adapter.

**Table 2.** The results of Ablation Study. Note the ‘WMS’ represents sample  $z$  without being modified by  $p$  and means  $z$  directly concatenate with  $p$ .

Uncertainty sample $z$	Position variant $p$	WMS	CMSM	LIDC-IDRI	REFUGE2
✓				0.862	0.824
	✓			0.866	0.827
✓	✓	✓		0.868	0.828
✓	✓		✓	<b>0.887</b>	<b>0.856</b>

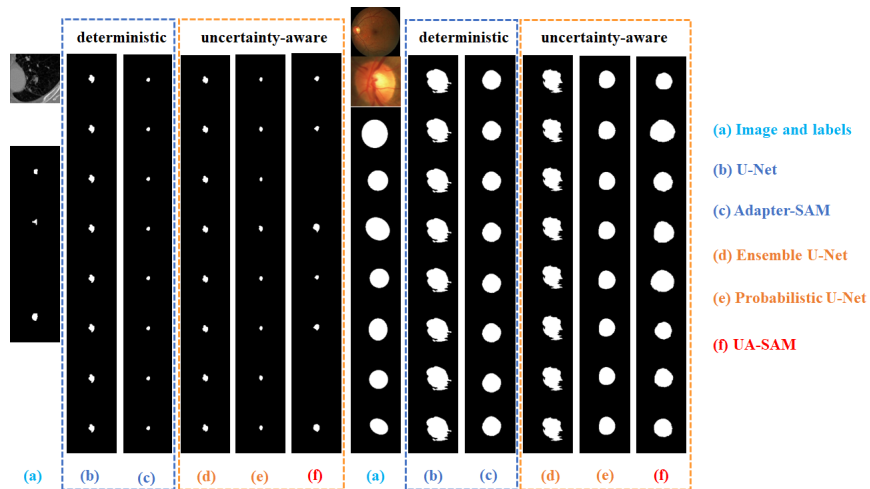


**Fig. 2.** Visualization results. On the left side is LIDC-IDRI, and on the right is REFUGE2 (raw and cropped images). The red text indicates the combined result with the uncertainty region for the best.

Furthermore, we compared several methods based on SAM from the Table. 2, we can see that there is no significant change in the model’s performance by utilizing a method similar to Prob U-Net, which directly concatenates the un-

certainty sample  $z$  into the Adapter. As we mentioned before, the model might ignore the uncertain sample. After incorporating the learnable position variant, the model only shows a slight performance improvement, with the greatest enhancement occurring when the uncertainty sample and position variant are added simultaneously. Our method utilizes position variant  $p$  as a condition to modify uncertainty sample  $z$ , which achieves improvements of 1.9% and 2.8%, respectively, on two datasets compared to the method of directly concatenating uncertainty sample and position variant. This confirms the effectiveness of the interaction method we proposed in UA-SAM. Fig. 2 shows the visualization results of UA-SAM and other methods. Our method can output more diverse segmentation masks closer to the label distribution than others, which is why UA-SAM performs better than when we conduct a majority vote strategy for both labels and prediction samples. It also demonstrates that the Uncertainty-aware Adapter we proposed can help SAM understand the uncertainty of medical images.

In addition, we retrained multiple UA-SAM models on the REFUGE2 dataset, only changing the dimensions of the latent space (the previous optimal model on REFUGE2 was the result of continuous training using the two datasets mentioned). From Fig. 3(a), We can observe that the optimal performance occurs when the latent space dimension is 6, which we chose before. Then, we compared the parameter of the Uncertainty-aware Adapter with the full fine-tune methods. The parameter count of the Uncertainty-aware Adapter is only 8.08M, which is much smaller than the others while outperforming others. It shows that our method is cost-efficient.

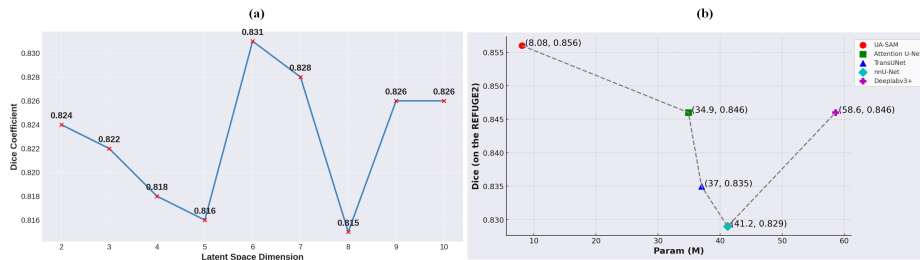


**Fig. 3.** Analytical experiments. (a) is the result of changing the latent space dimension. (b) is the comparison of models parameter.

## 4 Conclusion

In this paper, we propose a cost-efficient fine-tuning method called Uncertainty-aware Adapter, which can integrate medical domain knowledge and uncertainty inherent in medical images. By employing the condition-based interaction method between the Adapter and the sample from probabilistic latent space, our method



significantly improves over the original SAM, outperforming the SOTA on the LIDC-IDRI dataset and the REFUGE2 dataset. Furthermore, we clarified our method can output multiple likely segmentation hypotheses. We believe the uncertainty-aware method for fine-tuning SAM can make Segment 'Anything' more reliable, and it is indispensable for downstream medical tasks such as clinical diagnosis.

## References

- [1] Kirillov, A., Mintun, E., Ravi, N., Mao, H., Rolland, C., Gustafson, L., Xiao, T., Whitehead, S., Berg, A.C., Lo, W.Y., et al.: Segment anything. arXiv preprint arXiv:2304.02643 (2023)
- [2] Ma, J., He, Y., Li, F., Han, L., You, C., Wang, B.: Segment anything in medical images. *Nature Communications* **15**(1), 654 (2024)
- [3] Deng, R., Cui, C., Liu, Q., Yao, T., Remedios, L.W., Bao, S., Landman, B.A., Wheless, L.E., Coburn, L.A., Wilson, K.T., et al.: Segment anything model (sam) for digital pathology: Assess zero-shot segmentation on whole slide imaging. arXiv preprint arXiv:2304.04155 (2023)
- [4] Gao, Y., Xia, W., Hu, D., Gao, X.: Desam: Decoupling segment anything model for generalizable medical image segmentation. arXiv preprint arXiv:2306.00499 (2023)
- [5] Wu, J., Fu, R., Fang, H., Liu, Y., Wang, Z., Xu, Y., Jin, Y., Arbel, T.: Medical sam adapter: Adapting segment anything model for medical image segmentation. arXiv preprint arXiv:2304.12620 (2023)
- [6] Cheng, J., Ye, J., Deng, Z., Chen, J., Li, T., Wang, H., Su, Y., Huang, Z., Chen, J., Jiang, L., et al.: Sam-med2d. arXiv preprint arXiv:2308.16184 (2023)
- [7] Chen, T., Zhu, L., Deng, C., Cao, R., Wang, Y., Zhang, S., Li, Z., Sun, L., Zang, Y., Mao, P.: Sam-adapter: Adapting segment anything in underperformed scenes. In: *Proceedings of the IEEE/CVF International Conference on Computer Vision*. pp. 3367–3375 (2023)
- [8] Kohl, S., Romera-Paredes, B., Meyer, C., De Fauw, J., Ledsam, J.R., Maier-Hein, K., Eslami, S., Jimenez Rezende, D., Ronneberger, O.: A probabilistic u-net for segmentation of ambiguous images. *Advances in neural information processing systems* **31** (2018)
- [9] Bhat, I., Plum, J.P., Viergever, M.A., Kuijff, H.J.: Effect of latent space distribution on the segmentation of images with multiple annotations. *Machine Learning for Biomedical Imaging 2(UNSURE2022)*, 151–171 (Apr 2023)
- [10] Viviers, C.G., Valiuddin, A.M., de With, P.H., van der Sommen, F.: Probabilistic 3d segmentation for aleatoric uncertainty quantification in full 3d medical data. arXiv preprint arXiv:2305.00950 (2023)
- [11] He, K., Chen, X., Xie, S., Li, Y., Dollár, P., Girshick, R.: Masked autoencoders are scalable vision learners. In: *Proceedings of the IEEE/CVF conference on computer vision and pattern recognition*. pp. 16000–16009 (2022)

- [12] Vaswani, A., Shazeer, N., Parmar, N., Uszkoreit, J., Jones, L., Gomez, A.N., Kaiser, Ł., Polosukhin, I.: Attention is all you need. *Advances in neural information processing systems* **30** (2017)
- [13] Knegt, S.: Probabilistic-unet-pytorch (nov 2019), <https://github.com/stefanknegt/Probabilistic-Unet-Pytorch>
- [14] Fang, H., Li, F., Wu, J., Fu, H., Sun, X., Son, J., Yu, S., Zhang, M., Yuan, C., Bian, C., et al.: Refuge2 challenge: A treasure trove for multi-dimension analysis and evaluation in glaucoma screening. *arXiv preprint arXiv:2202.08994* (2022)
- [15] Ronneberger, O., Fischer, P., Brox, T.: U-net: Convolutional networks for biomedical image segmentation. In: *Medical Image Computing and Computer-Assisted Intervention–MICCAI 2015: 18th International Conference, Munich, Germany, October 5–9, 2015, Proceedings, Part III* 18. pp. 234–241. Springer (2015)
- [16] Isensee, F., Jaeger, P.F., Kohl, S.A., Petersen, J., Maier-Hein, K.H.: nnu-net: a self-configuring method for deep learning-based biomedical image segmentation. *Nature methods* **18**(2), 203–211 (2021)
- [17] Oktay, O., Schlemper, J., Folgoc, L.L., Lee, M., Heinrich, M., Misawa, K., Mori, K., McDonagh, S., Hammerla, N.Y., Kainz, B., et al.: Attention u-net: Learning where to look for the pancreas. *arXiv preprint arXiv:1804.03999* (2018)
- [18] Chen, J., Lu, Y., Yu, Q., Luo, X., Adeli, E., Wang, Y., Lu, L., Yuille, A.L., Zhou, Y.: Transunet: Transformers make strong encoders for medical image segmentation. *arXiv preprint arXiv:2102.04306* (2021)
- [19] Alom, M.Z., Hasan, M., Yakopcic, C., Taha, T.M., Asari, V.K.: Recurrent residual convolutional neural network based on u-net (r2u-net) for medical image segmentation. *arXiv preprint arXiv:1802.06955* (2018)
- [20] Chen, L.C., Zhu, Y., Papandreou, G., Schroff, F., Adam, H.: Encoder-decoder with atrous separable convolution for semantic image segmentation. In: *Proceedings of the European conference on computer vision (ECCV)*. pp. 801–818 (2018)
- [21] Yang, H., Wang, Q., Zhang, Y., An, Z., Chen, L., Zhang, X., Zhou, S.K.: Lung nodule segmentation and uncertain region prediction with an uncertainty-aware attention mechanism. *IEEE Transactions on Medical Imaging* (2023)
- [22] Ji, W., Yu, S., Wu, J., Ma, K., Bian, C., Bi, Q., Li, J., Liu, H., Cheng, L., Zheng, Y.: Learning calibrated medical image segmentation via multi-rater agreement modeling. In: *Proceedings of the IEEE/CVF Conference on Computer Vision and Pattern Recognition*. pp. 12341–12351 (2021)